The Barrel-Stave Model as Applied to Alamethicin and Its Analogs Reevaluated

D. R. Laver
Division of Neuroscience, John Curtin School of Medical Research, Australian National University, A.C.T., 2601, Australia

ABSTRACT Alamethicin and its analogs form cation selective, multi-conductance channels in lipid bilayers. The conductance levels have been thought to be due to a barrel-stave structure where conducting pores (barrels) are formed by the self-assembly of a variable number of α-helical rods (staves). The conductance transitions were then interpreted as the addition or deletion of peptide monomers from the pore-forming complex (Sansom, M.S. 1991. *Prog. Biophys. Mol. Biol.* 55:139–235). Initially, pore conductances were calculated from that expected of right circular cylinders of "bulk" electrolyte. More recent theories also included the access resistance of the electrolyte outside the pore. However, they all consistently overestimated the observed conductances. The reason for the discrepancy is presented here. Previous theories ignored the effects of ion concentration gradients near the pore. Hence, they only held in the limit of small bilayer potentials (<25 mV) and so would overestimate measurements that typically used much larger potentials (>100 mV). This theoretical flaw is corrected by using Läuger's theory of diffusion-limited ion flow (Läuger, P. 1976. *Biochim. Biophys. Acta.* 455:493–509). Thus, including the effects of ion concentration gradients results in a considerable improvement in predicting pore conductances. It is found that: 1) the effects of ion concentration gradients must be included in the barrel-stave model for it to apply to the available data; 2) previously published explanations for the discrepancy between the model and the data, namely the "distorted bundle" and the "head-to-tail aggregate" hypotheses are not necessary (reviewed by Sansom, 1991).

INTRODUCTION

Alamethicin and its analogs belong to the peptaibol family of channel-forming peptides. Alamethicin is a 20-residue peptide that adopts a α-helical conformation in lipid bilayers and aggregates to form cation selective, multi-conductance channels. It has been studied for over 20 years as a model for voltage-gated ion channels. The pattern of conductance levels formed by peptaibols is understood in terms of the barrel-stave model (Boheim, 1974; Bauman and Mueller, 1974), in which ion conducting pathways are formed by the self-assembly of parallel bundles of α-helical rods that line a cylindrical, electrolyte-filled pore. The peptides aggregate and dissociate to form circular bundles of different sizes. The conductance transitions observed in lipid bilayers are then interpreted as the addition or deletion of peptide monomers from the pore-forming complex.

The predicted conductances of these aggregates generally have been found to overestimate the observed values. The divergence between the model predictions and the data is more pronounced for larger aggregates (Sansom, 1991) and for shorter chain length peptaibols (Menestrina et al., 1986; Balaram et al., 1992) (Figs. 2–4). Menestrina et al. (1986) found that the short, 5-residue peptaibol, P5 and the 10-residue peptaibol, P10 had similar conductances, whereas the ion permeation model adopted predicted that P5 aggregates should have twice the conductance of P10 aggregates. To account for the discrepancy the authors proposed that P5 forms aggregates composed of head-to-tail linked α-helices. Sansom (1991) observed that his model predictions fitted well with the conductance levels for alamethicin and zervamicin (Zrv-IIB, a 16 residue peptaibol) for aggregates containing up to eight peptide monomers. Sansom (1991) and Balaram et al. (1992) proposed that larger aggregates must distort in the plane of the bilayer to produce an elliptical or "torpedo" cross section.

This paper evaluates the ion permeation models used in these studies. It provides a simple explanation for the discrepancies between the model predictions and the data, and it obviates the need for the above-mentioned proposals.

THEORY

The radius, r, of the pore formed by a bundle of n cylinders, of radius R, is given by Sansom (1991):

$$r = R[1/(\sin(\pi/n)) - 1] \quad (1)$$

In earlier studies the conductance, g_p, of these hypothetical aggregates were calculated by treating them as right circular cylinders, of length l, filled with an electrolyte with resistivity, ρ, equal to the bulk value (Hanke and Boheim, 1980; Boheim, 1983; Menestrina et al., 1986). Hence:

$$g_p = \pi r^2/l\rho \quad (2)$$

In more recent studies (Sansom, 1991; Balaram et al., 1992) calculations of pore conductance also include the electrical properties of the electrolyte outside the pore where the current paths converge at each pore mouth (i.e., the access resistance). The conductance of each external convergence region, g_a, is approximated by integrating the resistance of all electrolyte volume elements between the pore mouth and

Received for publication 27 August 1993 and in final form 2 November 1993.
Address reprint requests to D. R. Laver (using PO Box 334).

0006-3495/94/02/355/05 $2.00

an infinite hemisphere (Hall, 1975):

$$a_p = 4r/\rho \tag{3}$$

Thus the total conductance of the pore is due to the combination of the two convergence regions in series with the pore (Hille, 1992):

$$g_p = \frac{\pi r^2}{\rho}\left(1 + \frac{\pi r}{2}\right)^{-1} \tag{4}$$

For alamethicin $R = 0.5$ nm and $l = 3.0$ nm (Sansom, 1991). The predictions of Eq. 4 are compared with the conductances of various peptaibol aggregates in Figs. 2–4. Given the simplicity of the model it gives a surprisingly good account of the observed conductance levels. By comparing the relative contributions to the total conductance of the pore interior and the external convergence regions (cf. Eqs. 2 and 3) it can be seen that for larger aggregates the convergence regions dominate the electrical properties of the pore.

The above equations for pore conductance only hold in the limit of small membrane potentials, V, i.e. when $V \ll F/RT$. Herein lies the flaw in the model. The conductance measurements were all obtained using membrane potentials in excess of 100 mV, i.e. $V > 4 \times F/RT$. Under these conditions the ion concentrations in the vicinity of the pore markedly differ from those in the bulk solutions. Eqs. 5–7 are expressions for the current through the pore interior and convergence regions that include the effects of ion concentration gradients. They are adapted from the analysis of ion diffusion through pores by Läuger (1976). The current through the pore, I, given by Eq. 5 has a similar form to the Goldman equation:

$$I = \frac{\pi r^2}{l\rho} V_p \left\{ \frac{e^{((FV_1/RT))} \cdot e^{((FV_p/2RT))} - e^{((FV_2/RT))} \cdot e^{(-(FV_p/2RT))}}{e^{((FV_p/2RT))} - e^{(-(FV_p/2RT))}} \right\} \tag{5}$$

The electric potential difference between the ends of the pore, V_p, is related to the membrane potential by: $V_p = V + V_1 - V_2$ where V_1 and V_2 are the potential differences between the pore mouths and the bulk solutions (see Fig. 1). The relationship between the voltage drop across the external solutions and the current are given by Eqs. 6 and 7, which are derived from Eqs. B4 and B5 in Läuger (1976). Läuger's (1976) expression for the convergence permeabilities only considered the region of electrolyte between two hemispheres, one at the pore mouth and the other at infinity. To account for the region between the inner hemisphere and the flat disc at the more mouth an additional multiplying factor of $2/\pi$ was included in Läuger's equations (see Hille, 1992).

$$I = \frac{RT}{F}\frac{8r}{\rho}\{e^{((FV_1/RT))} - 1\} \tag{6}$$

$$I = \frac{RT}{F}\frac{8r}{\rho}\{1 - e^{((FV_2/RT))}\} \qquad g_p = \frac{I}{V} \tag{7}$$

$$C_1 = Ce^{((FV_1/RT))}\, C_2 = Ce^{((FV_2/RT))} \tag{8}$$

When the electric potentials V, V_1 and V_2 are small Eqs. 5–7 are the same as Eqs. 2 and 3. Eqs. 5–7 can be solved for

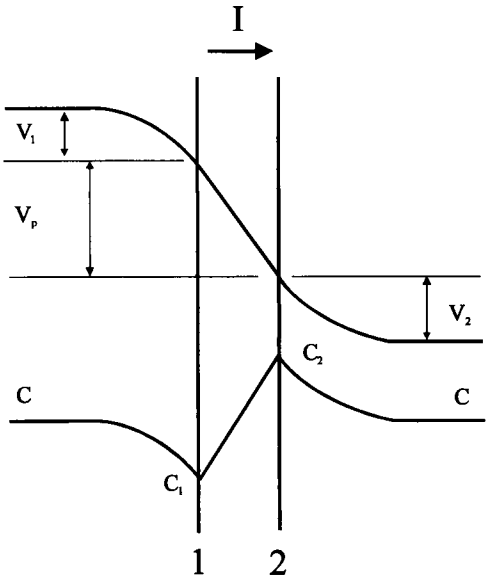

FIGURE 1 Schematic representation of the electric potential and ion concentration profiles across a diffusion-limited pore that passes a current I. Under these conditions the electric potentials and ion concentrations at the pore mouths (*1* and *2*) differ from their bulk values. At the left side of the pore, where the ions flows into the channel, the concentration of permeable ions reduces, whereas at the other end the concentration increases. Both the voltage drop across the external solutions and the local build up and depletion of ion concentrations reduce the driving force for ions within the pore.

I, V_1, and V_2. Values of g_p so calculated are compared with experimental observations in Figs. 2–4. The concentration of permeant ions at the pore mouths, C_1 and C_2, are related to the bulk concentration C by Eq. 8.

Fig. 2 shows the conductance levels of discrete bursts of zervamicin (Zrv-IIB) channels plotted against the expected number of helical peptides lining the pore. The data were obtained from Balaram et al. (1992), in which the conductances were measured using a trans-bilayer potential difference of 175 mV in symmetrical solutions containing 0.5 mol l^{-1} KCl. Using the same model parameters as used by Balaram et al. (1992), i.e. $l = 2.4$ nm, $R = 0.5$ nm, $\rho = 0.13$ Ωm the conductances predicted by Eqs. 1 and 5–7 are lower than those predicted by Eqs. 1–4 and also provide a better fit to the data. The parameters resulting from the solution to Eqs. 1 and 5–7 are summarised in Table 1. Fig. 3 shows a similar comparison of model predictions for conductance levels of alamethicin activity taken from Boheim (1974) using a bilayer potential of 100 mV in symmetrical 1.0 mol l^{-1} KCl solutions and Sansom (1991) using 125 mV in symmetrical 0.5 mol l^{-1} KCl solutions.

The effect of peptaibol chain length on the mean pore conductance is shown in Fig. 4. Menestrina et al. (1986) measured this using a bilayer potential in excess of 250 mV in symmetrical 1.0 mol l^{-1} KCl solutions. The predictions are shown of three models: 1) the model of Menestrina et al. (1986), in which access resistance was ignored; 2) the model including access resistance but excluding ion concentration gradients; and 3) the model proposed here, in which the effects of concentration gradients are included.

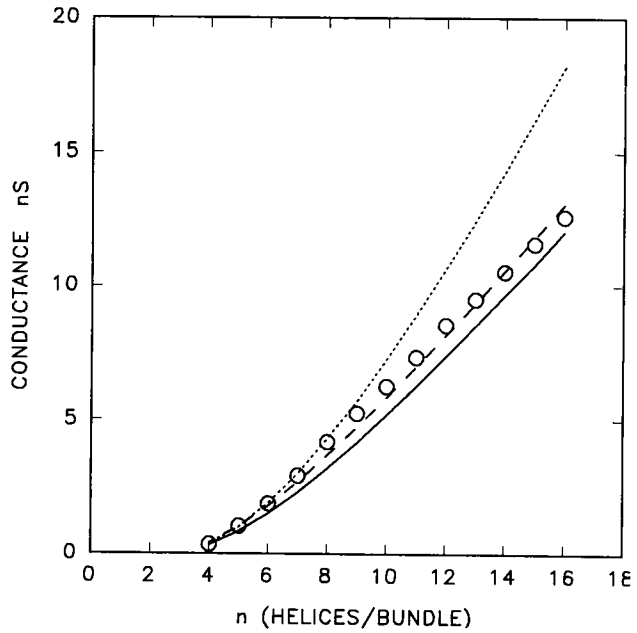

FIGURE 2 Conductance levels obtained from discrete burst of multilevel zervamicin (Zrv-IIB; ○) channels obtained from Balaram et al. (1992). These are plotted against the expected number of helical peptides lining the pore. Conductances were measured using a trans-bilayer potential difference of 175 mV in symmetrical solutions containing 0.5 mol l^{-1} KCl. (·····) The predictions of the model adopted by Balaram et al. (1992), in which the pore is modeled by a diffusion-limited, electrolyte-filled cylinder that ignores ion concentration gradients at the pore mouths (Eqs. 1–4); (——) the predictions of the corrected model, which is expanded to include the effect of ion concentration gradients (Eqs. 1 and 5–7); (– – –) the predictions of Eqs 1 and 5–7, except that the conductance of the pore interior is increased by 40%. The model parameters used here are the same as those used by Balaram et al. (1992): l = 2.4 nm, R = 0.5 nm, ρ = .13 ωm.

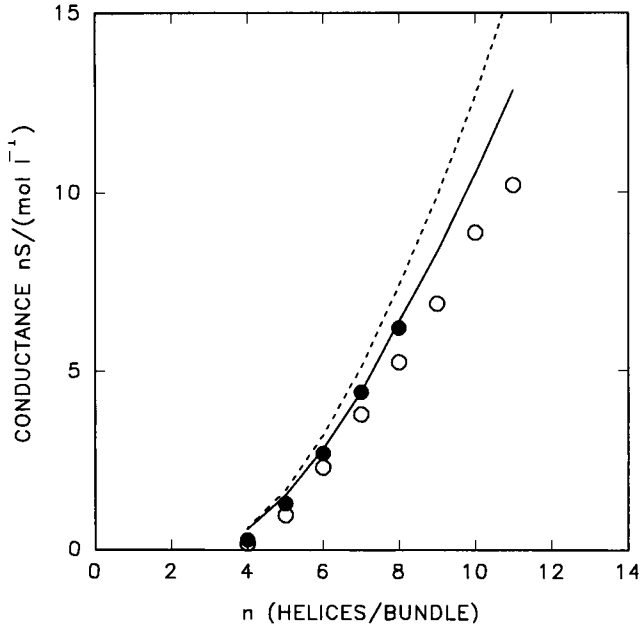

FIGURE 3 Conductance levels from discrete multilevel bursts of alamethicin activity in lipid bilayer taken from: (●) Boheim (1974) using a bilayer potential of 100 mV in symmetrical 1.0 mol l^{-1} KCl solutions; and (○) Sansom (1991) using 125 mV in symmetrical 0.5 mol l^{-1} KCl solutions. The conductance data shown here are normalized with respect to [KCl] so that both data sets can be compared to one set of calculations. The normalized conductances are plotted against the expected number of helical peptides lining the pore. The dashed line shows the predictions of Eqs. 1–4, and the solid line shows that of Eqs. 5–7.

TABLE 1 Parameters describing diffusion-limited ion flow in Zrv-IIB channels

n	g_P	V_1	V_2	C_1	C_2
	ns	*mV*		mol l^{-1}	
4	0.28	−6.0	5.2	.420	.573
8	2.84	−18.2	12.3	.309	.690
12	6.71	−26.9	15.5	.246	.753
16	11.17	−33.5	17.5	.207	.792

The parameter values were obtained from the solution of Eqs. 1 and 5–7, which is compared with the experimental data in Fig. 2. The data were obtained using a membrane potential of 175 mV in symmetrical solutions containing 0.5 mol l^{-1} KCl.

n is the number of helical peptides per pore forming bundle, g_P is the pore conductance in ns, V_1 and V_2 are the potential differences between the pore mouths and the bulk phases in mV (see Fig. 1), and C_1 and C_2 are the K^+ concentrations at each pore mouth in mol l^{-1} calculated using Eq. 8. The total voltage drop across the regions outside the pore ($V_2 - V_1$) is less than 30% of the membrane potential. For the larger peptide bundles [K^+] at the pore mouths results in a large concentration gradient across the pore that opposes the current flow.

DISCUSSION

When the intrinsic pore conductance is large the current becomes limited by the rate at which ions diffuse to and away from the pore mouths. Under these conditions the pore is diffusion-limited, and the electric potentials and ion concentrations at the pore mouths differ from their bulk values. At one end of the pore, where the ions flows into the channel, the concentration of permeable ions reduces, whereas at the other end the concentration increases (Fig. 1, Table 1).

For the case of alamethicin (l = 3.0 nm) the pore conductance exceeds the convergence conductance when the aggregates contain more than 15 peptides. Zrv-IIB, containing only 16 residues, form shorter (l = 2.4 nm), more conductive pores so that this condition is met for clusters of 12 or more (cf. Eqs. 2 and 3). The short synthetic peptide, P5 (l = .75–1.0 nm; Menestrina et al., 1986), only need form clusters of six to seven for this to occur. The divergence of the model, i.e., Eq. 4, from the data shown in Figs. 2 and 3 coincides with the onset of diffusion-limitation. This suggests that the main weakness of the model lies in its estimate of the convergence conductance rather than with the concept of an electrolyte-filled pore. A considerable improvement in the model predictions is achieved by including the effects of ion concentration gradients (Figs. 2 and 3). The remaining deviation from the data is probably due to simplicity of the ion permeation mechanism proposed for the pore interior, because merely adjusting ρ (Fig. 2) for the pore interior produced a good fit to the data.

Merely refining the model by altering the parameters is a pointless exercise, because other important factors are not included in the model. The ion permeation process in the

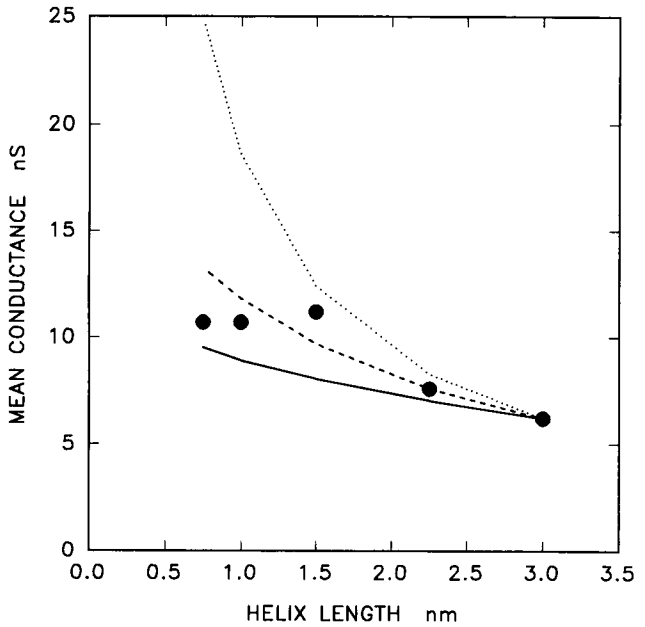

FIGURE 4 The mean conductance of discrete bursts of conductance activity due to short chain length peptaibols is plotted against their length. The data is taken from Menestrina et al. (1986). The conductances were measured using a bilayer potential in excess of 250 mV in symmetrical 1.0 mol l^{-1} KCl solutions. The datum points at 0.75 and 1.0 nm are from the one peptide (P5) and represent the limits in the uncertainty of its pore length. The dotted curve is the conductance-pore length relationship expected from a cylindrical pore (see Eq. 2). It is assumed that the pore length is equal to that of each peptide and that the different peptides form pores with identical average radii. The dashed curve shows the conductance predicted using Eq. 4, which includes the convergence conductance in the limit of small bilayer potentials. The full curve shows the conductance, including convergence conductance and ion concentration gradients (Eqs. 5–7).

smaller alamethicin aggregates is not like that in bulk electrolyte. The smaller aggregates produce narrow pores that exhibit specificity among monovalent cations (Hanke and Boheim, 1980), and their current-voltage characteristic in symmetrical solutions is superlinear (Gordon and Haydon, 1975). Their current-voltage characteristic can be interpreted by the peptide aggregates presenting an energy barrier to ion permeation. Thus ion-ion or ion-pore interactions play a significant role in the electrical properties of these pores. The larger pores are nonselective (Gordon and Haydon, 1975), and their current-voltage characteristic is linear. The interior of these pores behaves more like bulk electrolyte. Therefore, the model presented here is only suitable for describing the electrical properties of the larger polypeptide aggregates.

The more accurate version of the barrel-stave model presented here also provides an alternative explanation for the conductance properties of pores formed by the short synthetic polypeptide, P5. The conductance histograms for P5 (l = 0.75 nm), P10 (l = 1.5 nm), P15 (l = 2.2 nm), and P20 (l = 3.0 nm) reveal a broad distribution composed of indistinct peaks (Menestrina et al., 1986). The relative conductances of these pores were derived from their mean conductances assuming that the different peptaibols form aggregates of the same size. The conductance pore-length relationship was found to be much weaker than was predicted for an electrolyte-filled cylinder (Eq. 2; Fig. 4). These authors proposed that P5 peptides formed aggregates of head-to-tail dimers so that the predicted pore conductance could be halved. If one takes into account diffusion-limitation effects (Eq. 3), then a weaker relationship between pore length and conductance is predicted. This is because the conductance no longer depends entirely on the conductance of the pore interior. Once the effect of concentration gradients is included in the model, the dependence of conductance on pore length decreases even further (Fig. 4).

It can be seen in Fig. 4 that none of these models give a particularly satisfying account of the observations. However, given the uncertainty in the peptide aggregation number and the simplicity of the model, this is not surprising. The point to be stressed here is that a weak dependence of conductance on pore length, on its own, does not necessarily mean that the peptides form head-to-tail dimers. How then do short peptides produce membrane-spaning pores? An alternative to head-to-tail dimerization model is the concept of local "dimpling" of the bilayer to accommodate any length mismatch. Both models have been reviewed by Sansom (1991).

CONCLUSION

Presented here is a correction to a simple model, which results in a considerable improvement in predicting the conductance of pores formed by peptaibols. The effect of ion concentration gradients must be included in the barrel-stave model for it to correctly apply to the available data which have all been obtained using trans-pore potential differences well in excess of 25 mV. This work shows that the "distorted-bundle" and the "head-to-tail aggregate" hypotheses (see Introduction) are not necessary for explaining the observed conductance levels of peptaibol pores.

Detailed models for the geometric and electrostatic structures of alamethicin pores are now published and have been reviewed recently by Sansom (1993). The time is right to develop more sophisticated models for ion permeation through these channels. Such a model could be based on Levitt's (1991) continuum theory for multi-ion channels.

This work was supported by an Australian Research Council Senior Research Fellowship.

REFERENCES

Balaram, P., K. Krishna, M. Sukumar, I. R. Mellor, and M. S. Sansom. 1992. The properties of ion channels formed by zervamicins. *Eur. Biophys. J.* 21:117–128.

Baumann, G., and Mueller, P. 1974. A molecular model of membrane excitability. *J. Supramol. Struct.* 2:538–557.

Boheim, G. 1974. Statistical analysis of alamethicin channels in black lipid membranes. *J. Membr. Biol.* 19:277–303.

Gordon, L. G., and D. A. Haydon. 1975. Potential-dependent conductances in lipid membranes containing alamethicin. *Philos. Trans R. Soc. Lond. B. Biol. Sci.* 270:433–447.

Hall, J. E. 1975. Access resistance of a small circular pore. *J. Gen. Physiol.* 66:531–532.

Hanke, W., and G. Boheim. 1980. The lowest conductance state of the alamethicin pore. *Biochim. Biophys. Acta.* 596:456–462.

Hille, B. 1992. Ionic channels of excitable membranes. Ed. 2. Sinaurer Associates Inc., Sunderland, MA.

Läuger, P. 1976. Diffusion-limited ion flow through pores. *Biochim. Biophys. Acta.* 455:493–509.

Levitt, D. G. 1991. General continuum theory for multiion channel. I. Theory. *Biophys. J.* 59:271–277.

Menestrina, G., K.-P. Voges, G. Jung, and G. Boheim. 1986. Voltage-dependent channel formation by rods of helical polypeptides. *J. Membr. Biol.* 93:111–132.

Sansom, M. S. 1991. The biophysics of peptide models of ion channels. *Prog. Biophys. Mol. Biol.* 55:139–235.

Sansom, M. S. P. 1993. Alamethicin and related peptaibols-model ion channels. *Eur. Biophys. J.* 22:105–124.